A tunable diode laser study of the reactions of nitric and nitrous acids: HNO_3+NO and HNO_2+O_3

G. E. Streit[a] and J. S. Wells

Time and Frequency Division, National Bureau of Standards and Physics Department, University of Colorado, Boulder, Colorado 80303

F. C. Fehsenfeld and Carleton J. Howard

Aeronomy Laboratory, NOAA Environmental Research Laboratories, Boulder, Colorado 80303
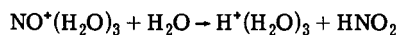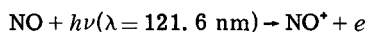(Received 13 November 1978)

This study of the reactions of nitrous and nitric acids demonstrates a new application of tunable diode laser technology. The diode laser is used for the direct detection of HNO_2 and HNO_3 in a chemical kinetic system. We have established an upper limit for the rate constant for $HNO_3 + NO \rightarrow HNO_2 + NO_2$ $[k_1 \le (3.4 \pm 2) \times 10^{-22}$ cm^3/molecule·s] and have confirmed that nitrous acid is a product of this reaction. We have also established an upper limit for the rate constant for $HNO_2 + O_3 \rightarrow HNO_3 + O_2 [k_4 \le (4.5 \pm 3) \times 10^{-19}$ cm^3/molecules].

INTRODUCTION

Nitrous and nitric acids are present throughout the atmosphere and play a role in atmospheric chemistry which has not yet been fully determined. Nitric acid is a long recognized tropospheric constituent[1] and has also been positively identified in the stratosphere[2,3] where it serves as a sink for NO_x.[4] Nitrous acid is a potential source of hydroxyl radicals in the troposphere through the photolytic reactions[5]

$$HNO_2 + h\nu \begin{array}{c} \xrightarrow{\lambda < 585 \text{ nm}} HO + NO \\ \xrightarrow{\lambda < 366 \text{ nm}} H + NO_2 \end{array}$$
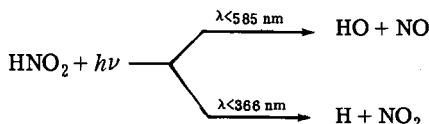
Nitrous acid is also produced in the D region of the ionosphere through the ion–molecule reaction sequence[6]:

$$NO + h\nu(\lambda = 121.6 \text{ nm}) \rightarrow NO^+ + e$$

$$NO^+ + 3H_2O \xrightarrow{M} NO^+(H_2O)_3 \text{ (Three sequential hydrations)}$$

$$NO^+(H_2O)_3 + H_2O \rightarrow H^+(H_2O)_3 + HNO_2$$

The possibility that nitrous acid might enter into the stratospheric ozone cycle led us to initiate a study of its spectroscopy and chemistry. The use of a tunable diode laser in the 6 μm region which overlaps both the ν_2 band of HNO_2 ($N = 0$ stretch) and the ν_2 band of NHO_3 (NO_2 asymmetric stretch) yields the distinct advantage of directly and unambiguously detecting both species. Since the conversion of nitric acid to nitrous acid was considered as a source of HNO_2, the reactions $NHO_3 + NO$ and $HNO_3 + HNO_2$ were also studied to gain better understanding of the mixed acid system.

EXPERIMENTAL

A block diagram of the experimental apparatus indicating the diode laser and a 12 l Pyrex static reactor is shown in Fig. 1a. A 50 cm absorption cell was used in place of the static reactor for spectroscopic identification and sensitivity measurements. The gas handling system for the $HNO_2 + O_3$ reaction was more complicated and is shown in Fig. 1b.

A tunable lead sulfide selenide diode laser which covered the spectral region of interest in a semicontinuous manner was the central component of the system. The laser was operated on a liquid helium cooled heat sink and controlled by a power supply unit with an integral function generator which provides both current sweep and modulation modes of operating the laser. The output power of about 2 mW was generally distributed over several modes which were separated by about 1 cm^{-1}. A single mode was selected with a 0.8 m monochromator and typically the mode which emerges from the monochromator had about 100–200 μW, of power depending upon the frequency. The linewidth of this mode was less than 10^{-4} cm^{-1} (3 MHz).

A linear spectrum spanning from less than 0.01 cm^{-1} to approximately 1 cm^{-1} could be displayed on the oscilloscope by operating the laser with a variable amplitude, low-frequency sawtooth modulation. The same linear spectrum could also be used for absorption measurements by slowly sweeping the laser frequency while mechanically chopping the laser beam and using phase sensitive detection as shown in Fig. 2a. By using an external high frequency low amplitude modulation in combination with the sweep mode on the laser controller, a derivative display of the spectrum could be obtained as shown in Fig. 2b. In our kinetic measurements a single rovibronic line that was both strong and free from interference from other absorption was selected to monitor the relative concentrations of the acids.

Two very important aspects of a kinetic study in a static reactor are linearity of signal vs concentration and stability of reactants in the cell. Figure 3 shows the linearity of HNO_3 signal for concentrations from 1×10^{15} to 8×10^{15} molecule/cm^3. A mixture of 7.3×10^{15} molecule/cm^3 HNO_3 in 3.5×10^{17} molecule/cm^3 N_2 remained very stable in the reactor over a period of greater than 1 h. Nitrous acid, however, when produced in concentrations typically used in kinetic runs, decayed by ap-

proximately 40% in a period of 1 h. Therefore, kinetic measurements involving nitrous acid were restricted to intervals of 2–3 min so that the decomposition of nitrous acid would be negligible.

Several sources of nitrous acid were used. The first, which provided calculable HNO_2 concentrations,[7] was an *in situ* preparation performed by mixing NO, H_2O, and NO_2 in known concentrations. The second was a liquid generator containing a mixture of a saturated solution of KNO_2 (70%) and one normal HCl (30%). Nitrous acid could be obtained from this generator either by pumping off the vapor or by bubbling HCl gas through the solution. The water vapor concentration in the evolved gas stream was substantially reduced by passing the gas stream through a trap at $-7\,^\circ C$. The third method was a solid generator in which HCl vapor was passed through a trap containing solid KNO_2. However, this method was found to be sensitive to the amount of moisture in the KNO_2. When totally dry, the efficiency of HNO_2 production fell substantially.

Anhydrous nitric acid was prepared by vacuum distillation of reagent grade HNO_3 (16 M) from an excess of reagent grade concentrated sulfuric acid (18 M). The distilled HNO_3 was passed over $CaSO_4$ and was stored in the dark at $-77\,^\circ C$. CP grade NO ($>99\%$) was used after passing it through a silica gel trap at $-77\,^\circ C$.

Kinetic measurements were made by first injecting a small amount of HNO_3 or HNO_2 into the reactor. The initial acid concentration was determined by pressure measurement with a capacitance manometer. The stability of the injected sample was monitored by repetitively scanning one of the absorption features as described earlier. Then the second reactant, NO or an O_3/Ar mixture, was injected through a glass tube extending nearly to the center of the reactor. The outlets on this tube were shaped like small jets to provide rapid turbulent mixing of the two reactants. The change in acid concentration was then observed by continued scanning of the absorption line at measured time intervals.

The measured rate constants were taken as upper limits. There was no dependence of the rate constants on reactor pressure and no indication that the reactions were heterogeneous or diffusion controlled. However, since only one size reactor was used, we are not certain that the measured values are the purely homogeneous rate constants.
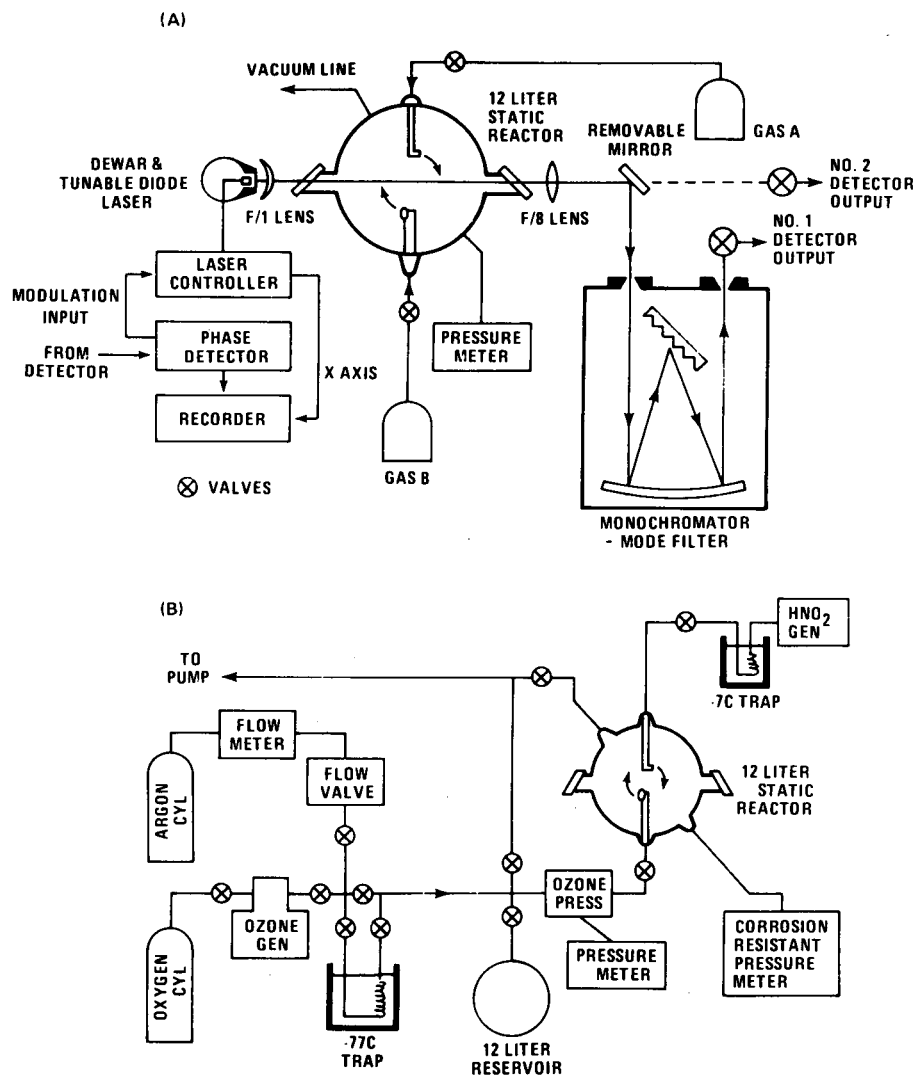

FIG. 1. (a) Diagram of apparatus used for HNO_2 and HNO_3 detection and kinetic studies. The lead sulfide selenide diode laser is in a liquid helium dewar and is shown to the left of the reactor. The controller is the laser power supply control unit. The phase detector supplies the reference modulation signal to the controller and provides phase sensitive detection of the absorption signal from the detector after the monochromator. Absorption signals are monitored on an $X-Y$ recorder. The inlets on the reactor are designed to enhance mixing of the injected reactants. (b) Diagram of a apparatus showing details of the gas handling system used to study the $HNO_2 + O_3$ reaction. Mixtures of ozone and argon were prepared in the 12 l reservoir and added to the reactor after the HNO_2. The ozone was stored on dry ice cooled silica gel. The ozone concentration used in the kinetic runs was measured after the run as described in the text.
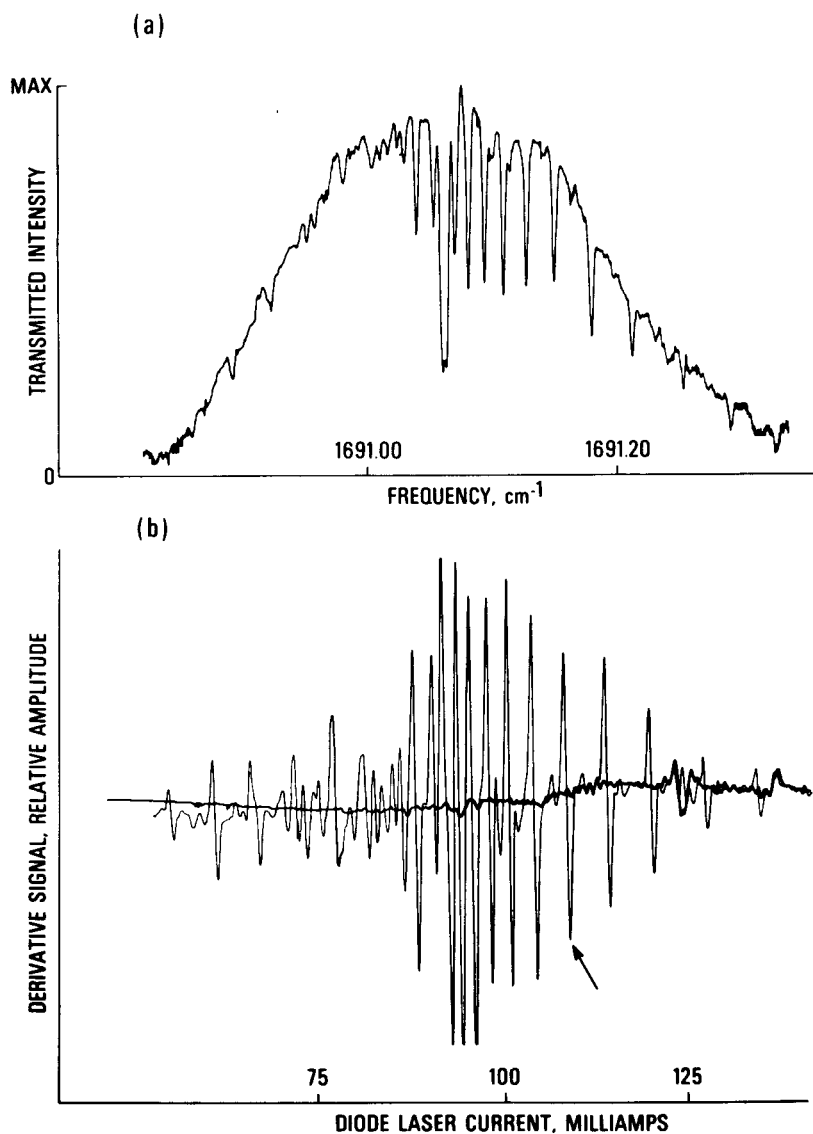
(a)

FIG. 2. (a) A segment of the
HNO$_3$ spectrum obtained by
mechanically chopping the laser
beam and processing the de-
tected signal through a phase
detector. The HNO$_3$ concen-
tration was about 10^{16} mole-
cule/cm^3. The envelope of the
spectrum is the transmission
of the monochromator which is
determined primarily by the
exit aperture and a large area
detector. This group of lines
is one of a series of similar
clusters of lines spaced about
0.4 cm^{-1} apart over a 60 cm^{-1}
interval. The estimated accu-
racy of the frequency scale is
± 0.03 cm^{-1}. (b) Derivative
spectrum of about 5 × 10^{15} mole-
cule/cm^3 of HNO$_3$. Traces are
shown for both empty and filled
cell. The arrow indicates a
typical line (reasonably well
isolated and in the linear re-
gime) chosen for monitoring in
a kinetic run.

The ozone concentrations were measured by UV ab-
sorption at 254 nm. All measurements were made at
296 ± 2 °K.

RESULTS

A. HNO$_3$ + NO → HNO$_2$ + NO$_2$ (1)

The measurement data for the reaction of HNO$_3$ with
NO are summarized in Table I. The initial HNO$_3$ con-
centration [HNO$_3$]$_0$, was varied from (2 to 17) × 10^{15} mol-
ecule/cm^3 and the NO concentration was varied from
(8 to 150) × 10^{16} molecule/cm^3. The ratio [NO]/[HNO$_3$]$_0$
ranged from about 12 to 220, therefore, the bimolecu-
lar reaction was pseudo-first-order in HNO$_3$. The data
for experiments 2 through 4 are given in Fig. 4, where
log[HNO$_3$] is shown as a function of reaction time. We
observe a downward curvature in all of the data. From
the initial slopes one estimates the reaction rate con-
stant to be, $k_1' \simeq 7 \times 10^{-22}$ cm^3/molecule · s. However,
the HNO$_2$ product of the reaction also reacts with HNO$_3$,

$$HNO_2 + HNO_3 \rightarrow H_2O + 2NO_2 \qquad (2)$$
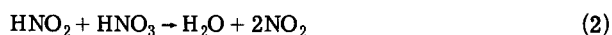
with a rate constant $k_2 \simeq 1.6 \times 10^{-17}$ cm^3/molecule · s, [8]

which is more than 10^4 times faster than the primary
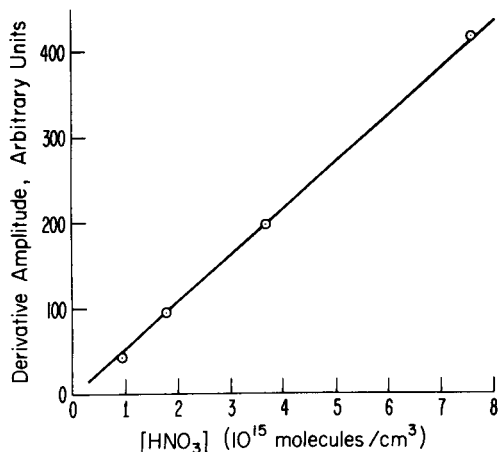process. Including this secondary reaction, a simple

FIG. 3. Plot of signal strength (peak to peak derivative signal
amplitude) versus HNO$_3$ concentration for the concentration
range used in this work. A constant concentration of N$_2$ of
about 3 × 10^{17} molecule/cm^3 was maintained in the reactor.

TABLE I. Rate constant measurements for the reaction $HNO_3 + NO$.

Exp. No.	$[HNO_3]_0$ $(10^{15}$ molecule/cm$^3)$	$[NO]$ $(10^{16}$ molecule/cm$^3)$	k $(10^{-22}$ cm^3/molecule $\cdot$ s)
1	5.6	30.8	3.3
2	6.7	8.1	3.7
3	5.6	59.3	3.2
4	6.3	136	2.8
5	17.1	146	3.9
6	2.6	42.9	3.8
7	1.9	18.6	4.1
8	16.3	34.3	2.0

Average (std. dev.) $\pm$ estimated error $= [3.4 \, (0.7) \pm 2] \times 10^{-22} \dfrac{cm^3}{molecule \cdot s}$

steady state analysis with $d[HNO_2]/dt = 0$ predicts that rate constants derived from the initial slope are equal to $2k_1$. Thus the observed rate of removal of HNO_3 is twice the rate of Reaction (1) because of the very rapid destruction of a second HNO_3 molecule by the HNO_2 product. The overall process is:

$$NO + 2HNO_3 \rightarrow H_2O + 2NO_2 .$$
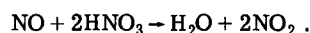
The downward curvature of the data in Fig. 4 indicates that there is additional secondary chemistry removing nitric acid. This is not surprising because the relatively large initial concentration of HNO_3 generates large amounts of NO_2 and H_2O products that are reactive in the NO and HNO_3 mixtures, through both homogeneous and heterogeneous mechanisms. Reaction (1) is nearly thermoneutral,[9] $\Delta H^0_{298} = 0.1$ kcal/mole, $\Delta S^0_{298} = 2.9$ e.u. and $K_{eq} = 3.6$. The large excess concentration of NO and the destruction of the HNO_2 product by Reaction (2) inhibits obtaining equilibrium in the observation periods used in our study. However, the upper limit rate constant reported in Table I, $k_1 \leq 3.4 \times 10^{-22}$

cm^3/molecule $\cdot$ s, can be used to place an upper limit on the reverse reaction:

$$HNO_2 + NO_2 \rightarrow HNO_3 + NO , \qquad (3)$$

$k_3 \leq 1 \times 10^{-22}$ cm^3/molecule $\cdot$ s.

The HNO_2 product of Reaction (1) was detectable only in experiments with very small HNO_3 concentrations. Thus HNO_2 absorption features would appear at long reaction times when the HNO_3 concentration had decayed significantly or in experiments with very small initial HNO_3 concentrations.

B. $HNO_2 + O_3 \rightarrow HNO_3 + O_2$ (4)

Due to a failure of the 6 μm diode laser used in the HNO_3 studies, the HNO_2 reaction measurements were made using a second diode laser operating in the 1225–1250 cm^{-1} region.

The measurement data for this reaction are summarized in Table II. The initial HNO_2 concentration was not measured accurately but was estimated to be in the range $(5-30) \times 10^{14}$ molecule/cm^3. The HNO_2 concentration was observed to decay by a factor of 2–5 in most of the measurements.

Interfering chemistry was a serious limitation during this study because it was not possible to produce HNO_2 without large quantities of attendant NO, NO_2, and H_2O. It was found that substantial amounts of ozone were lost to interfering reactions, e.g.,

$$NO + O_3 \rightarrow NO_2 + O_2 \qquad (5)$$

and

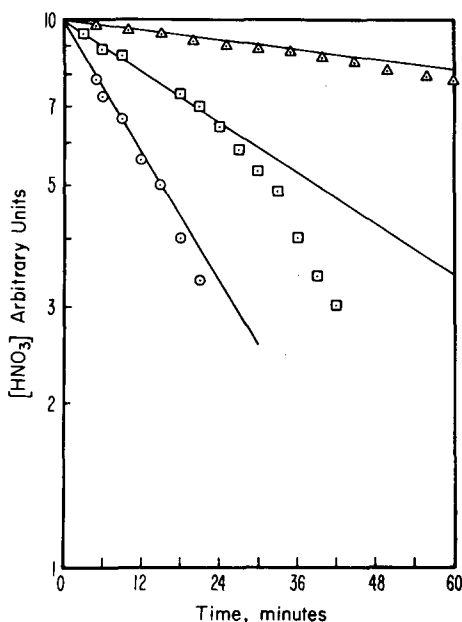$$NO_2 + O_3 \rightarrow NO_3 + O_2 . \qquad (6)$$

FIG. 4. Typical data for kinetic measurements. The slopes of the lines are the first order rate constants. These divided by the NO concentration are equal to $2k_1$ as described in text. See Table I for conditions: $\triangle$ = exp. 2, $\square$ = exp. 3, and $\circ$ = exp. 4.

TABLE II. Rate constant measurements for the reaction $HNO_2 + O_3$.

| Exp. No.	$[O_3] \, (10^{16}$ molecule/cm$^3)$	$k \, (10^{-19}$ cm^3/molecule $\cdot$ s)
1	1.6	3.4
2	2.5	3.8
3	2.6	5.7
4	5.3	5.3
5	1.3	4.4
6	2.7	4.1

Average (std dev) $\pm$ estimated error $= [4.5 \, (0.9) \pm 3] \times 10^{-19}$ cm^3/molecule $\cdot$ s .

These reactions were rapid on the time scale of the experiment and destroyed between 20% and 50% of the ozone that was initially injected into the reactor. The ozone concentrations shown in Table II were used to calculate the rate constants and were obtained from measurements on the gas in the reactor after the rate measurement was completed.

The unknown concentrations of impurities and HNO_2 initially present in the reactor make it impossible to evaluate the role of secondary chemistry in the HNO_2 + O_3 reaction studies. Slight downward curvature of the plots of $[HNO_2]$ vs reaction time was observed similar to that shown in the HNO_3 data in Fig. 4. HNO_3 was not detected with the 1230 cm^{-1} laser, although one expects it to be present in the reactor either as a product of Reaction (4) or as a product of the reaction of nitrogen oxides, particularly N_2O_5 with H_2O on the surface of the reactor. The rate constant in Table II has not been corrected for possible secondary chemistry and, therefore, must be strictly considered an upper limit.

C. $HNO_2 + HNO_3 \rightarrow H_2O + 2NO_2$ (2)

One measurement was made to confirm that this reaction was indeed rapid relative to the other reactions studied. About 9.5×10^{16} molecule/cm^3 of HNO_3 was added to the reactor containing about 3×10^{15} molecule/cm^3 of HNO_2. The HNO_2 decay was exponential for the 5 s observation period and yielded a rate constant of 1.1×10^{-17} cm^3/molecule·s. The rate constant combined with the thermochemistry for the reaction[9] ΔH^0_{298} $= + 8.4$ kcal/mol and $\Delta S^0_{298} + 36.4$ e.u., and $K_{eq} = 1.4$ $\times 10^{21}$ molecule/cm^3 can be used to estimate the rate constant for the reverse reaction:

$$H_2O + 2NO_2 \rightarrow HNO_2 + HNO_3$$ (7)

$k_7 \approx 8 \times 10^{-39}$ cm^6/molecule^2·s.
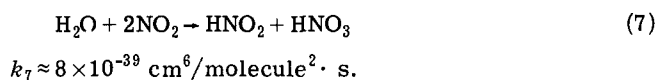
DISCUSSION

Early investigations by Jaffe and Ford[10] and Smith[11] of the HNO_3 + NO reaction were complicated by the necessity of using NO_2 production as an indirect indicator and were inconclusive as to the mechanism and detailed rate constants. A more recent measurement by Kaiser and Wu[8] of 1.5×10^{-20} cm^3/molecule·s was complicated by a very high surface to volume ratio (0.63 cm^{-1}) and was given as an upper limit for the homogeneous reaction. Our measurement, in a reactor of surface to volume ratio (s/v) 0.21 cm^{-1} reduces this limit by nearly two orders of magnitude. While it still must be regarded as an upper limit, the demonstrated stability of reactants in the reactor and the fact that no pressure dependence was observed over a twenty fold range of pressure gives evidence that the measurement should be near the true homogeneous rate.

There are two reported rate constants for the reaction between nitrous and nitric acids. Kaiser and Wu[8] report a value of $(1.55 \pm 0.3) \times 10^{-17}$ cm^3/molecule·s in their system with s/v equal to 0.63 cm^{-1}. The limit is one standard deviation. England and Corcoran,[12] in an

indirect study, report a value of 0.97×10^{-17} cm^3/molecule·s measured in a system with s/v equal to 0.355 cm^{-1}. Our measurement of $k_2 = 1.1 \times 10^{-17}$ cm^3/molecule·s agrees remarkably well with the previous reports and seems to indicate that the process is homogeneous.

The nitrous acid–ozone reaction was potentially the most interesting for stratospheric chemistry, but the very low rate constant measured in this work, (4.5 ± 3) $\times 10^{-19}$ cm^3/molecule·s, substantially decreases the importance of that reaction. The inherent instability of the reactants and the presence of H_2O, NO, and NO_2 in the reactor lead to the large error limits quoted.

This work demonstrates the versatility of the tunable diode laser by using it for direct detection of nitrous and nitric acids in a kinetic measurement system. We estimate that a 100 fold improvement in sensitivity is possible by using a conventional multipass or White cell configuration. With increased sensitivity the study of the chemistry of labile species will be possible. We also plan to extend the technique to a flow system for measurements of fast reactions.

The diode laser also provides high resolution spectra which were previously unavailable and which are unambiguous molecular signatures for analysis of the composition of multicomponent gas mixtures. Recent high resolution measurements on the atmospheric molecules ClO,[13] HNO_3,[14] and HOCl[15] suggest a promising future for this technology.

[1]P. A. Leighton, *The Photochemistry of Air Pollution.* (Academic, New York, 1961).
[2]D. G. Murcray, T. G. Kyle, F. H. Murcray, and W. J. Williams, J. Opt. Soc. Am. **59**, 1131 (1969).
[3]A. L. Lazrus, B. Gandrud, and R. B. Cadle, J. Appl. Meteorol. **11**, 389 (1972).
[4]H. S. Johnston, Science **173**, 517 (1971).
[5]R. A. Cox, J. Photochem. **3**, 175 (1974).
[6]F. C. Fehsenfeld and E. E. Ferguson, J. Geophys. Res. **74**, 2217 (1969).
[7]W. H. Chan, R. J. Nordstrom, J. G. Calvert, and J. H. Shaw, Environ. Sci. Technol. **10**, 674 (1976).
[8]E. W. Kaiser and C. H. Wu, J. Phys. Chem. **81**, 187 (1977).
[9]S. W. Benson, *Thermochemical Kinetics* (Wiley, New York, 1976), p. 290–295.
[10]S. Jaffe and H. W. Ford, J. Phys. Chem. **71**, 1832 (1967).
[11]J. H. Smith, J. Amer. Chem. Soc. **69**, 1741 (1947).
[12]C. England and W. H. Corcoran, Ind. Eng. Chem. Fundam. **13**, 373 (1975).
[13]R. T. Menzies, J. S. Margolis, E. D. Hinkley, and R. A. Toth, Appl. Opt. **16**, 523 (1977).
[14]A. Maki and J. S. Wells, J. Mol. Spectrosc. (submitted).
[15]R. L. Sams, private communication.